

Supporting Information

Solar-Assisted All-Solid Supercapacitors by Composite Nanostructure of ZnO Nanowires with GO and rGO

Cigdem Tuc Altaf,^[a] Arpad Mihai Rostas,^[b] Maria Mihet,^[b] Mihaela Diana Lazar,^[b] Igor Iatsunskyi,^[c] Emerson Coy,^[c] Emre Erdem,^[d] Mehmet Sankir,^[a] Nurdan Demirci Sankir,^[a]

^[a] Department of Materials Science and Nanotechnology Engineering, TOBB University of Economics and Technology, Sogutozu Caddesi No 43 Sogutozu 06560 Ankara, Turkey

^[b] National Institute for Research and Development of Isotopic and Molecular Technologies- INCDTIM, 67-103 Donat, 400293 Cluj-Napoca, Romania

^[c] NanoBioMedical Centre, Adam Mickiewicz University in Poznań, Wszechnicy Piastowskiej 3, 61-614, Poznań, Poland

^[d] Faculty of Engineering and Natural Sciences, Sabancı University, Orhanli, Tuzla, 34956, Istanbul, Turkey

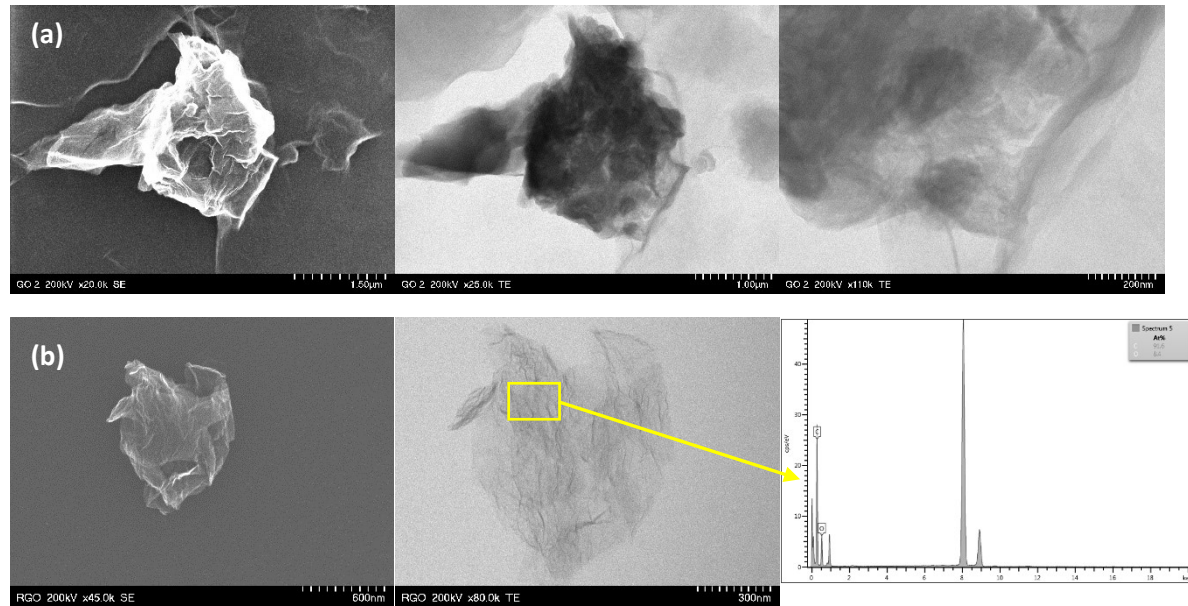


Figure S1. SEM/TEM images of pristine (a) GO and (b) rGO used for the preparation of GO/ZnO NW, and rGO/ZnO NW composites. (The difference in transparency for the two samples is a visible indication of the difference in the number of Carbon layers, that is GO is less transparent since it has 9 C layers, compared to rGO which shows only 3 C layers. The number of C layers was estimated from XRD data.)

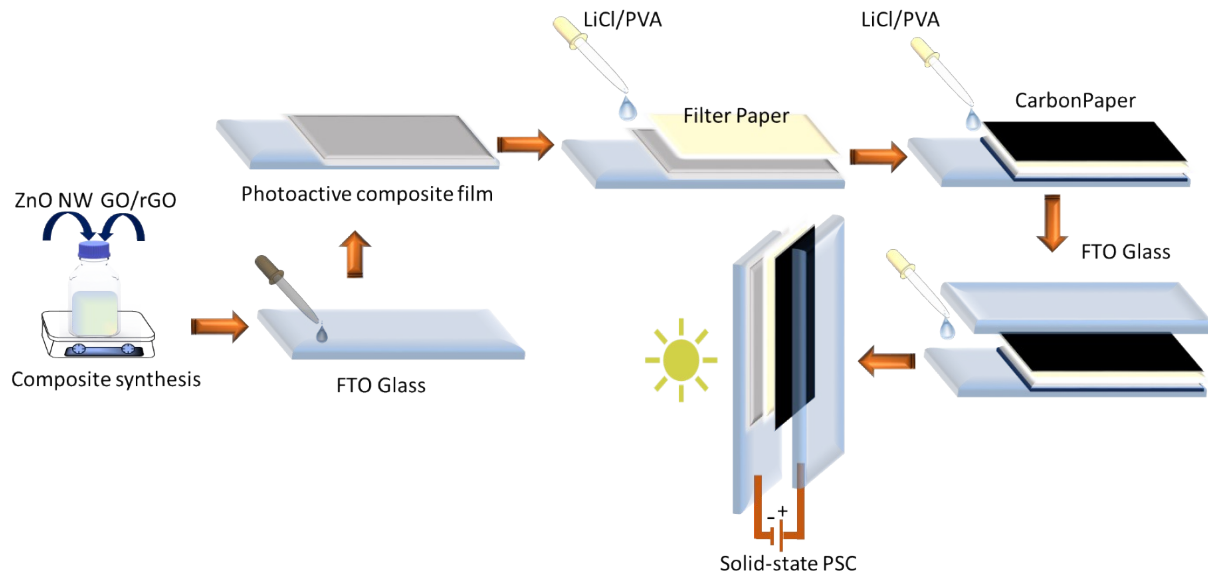


Figure S2. Schematic representation of PSC preparation route.

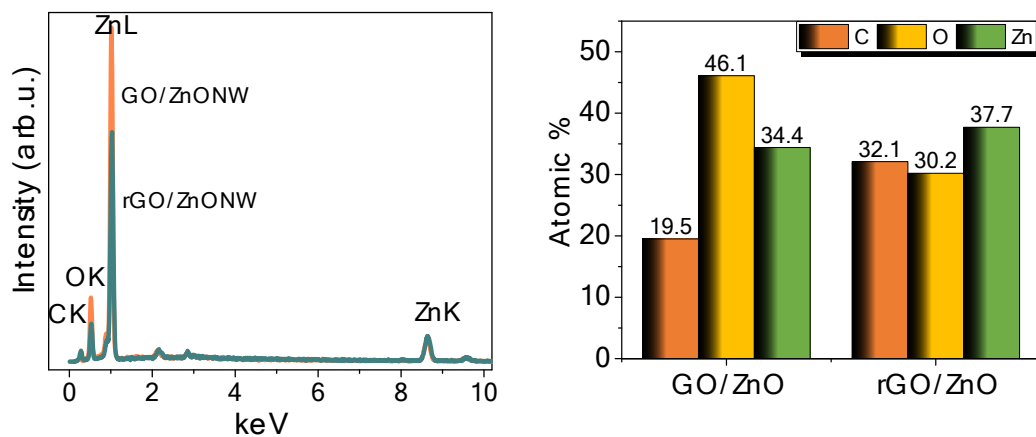


Figure S3. EDS spectra and atomic percentage (%) of the composite powders

CV Measurements

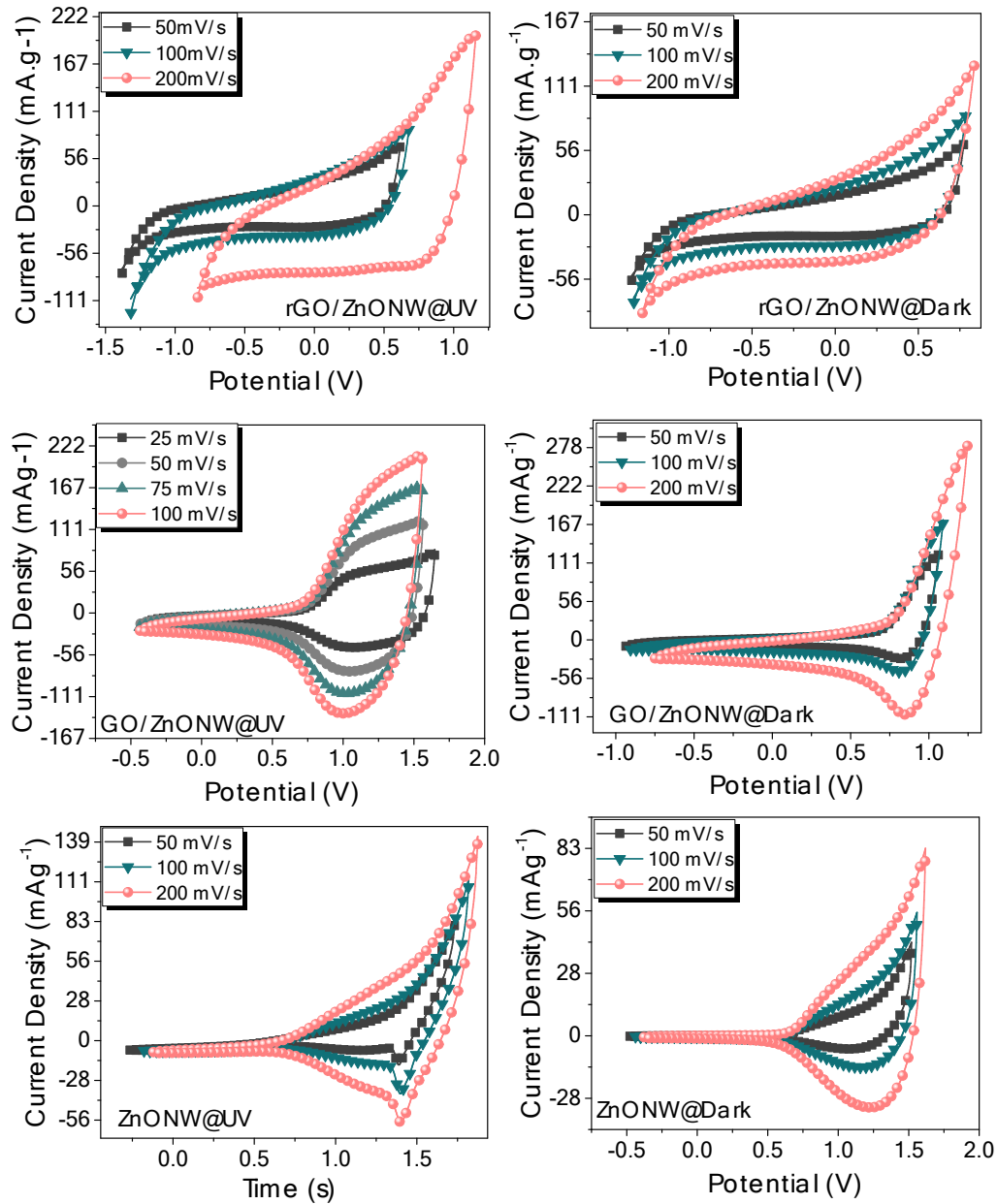


Figure S4. CV curves of the composite and pristine ZnO NW-based PSC devices at various current densities

GCD curves for composite P-SCs

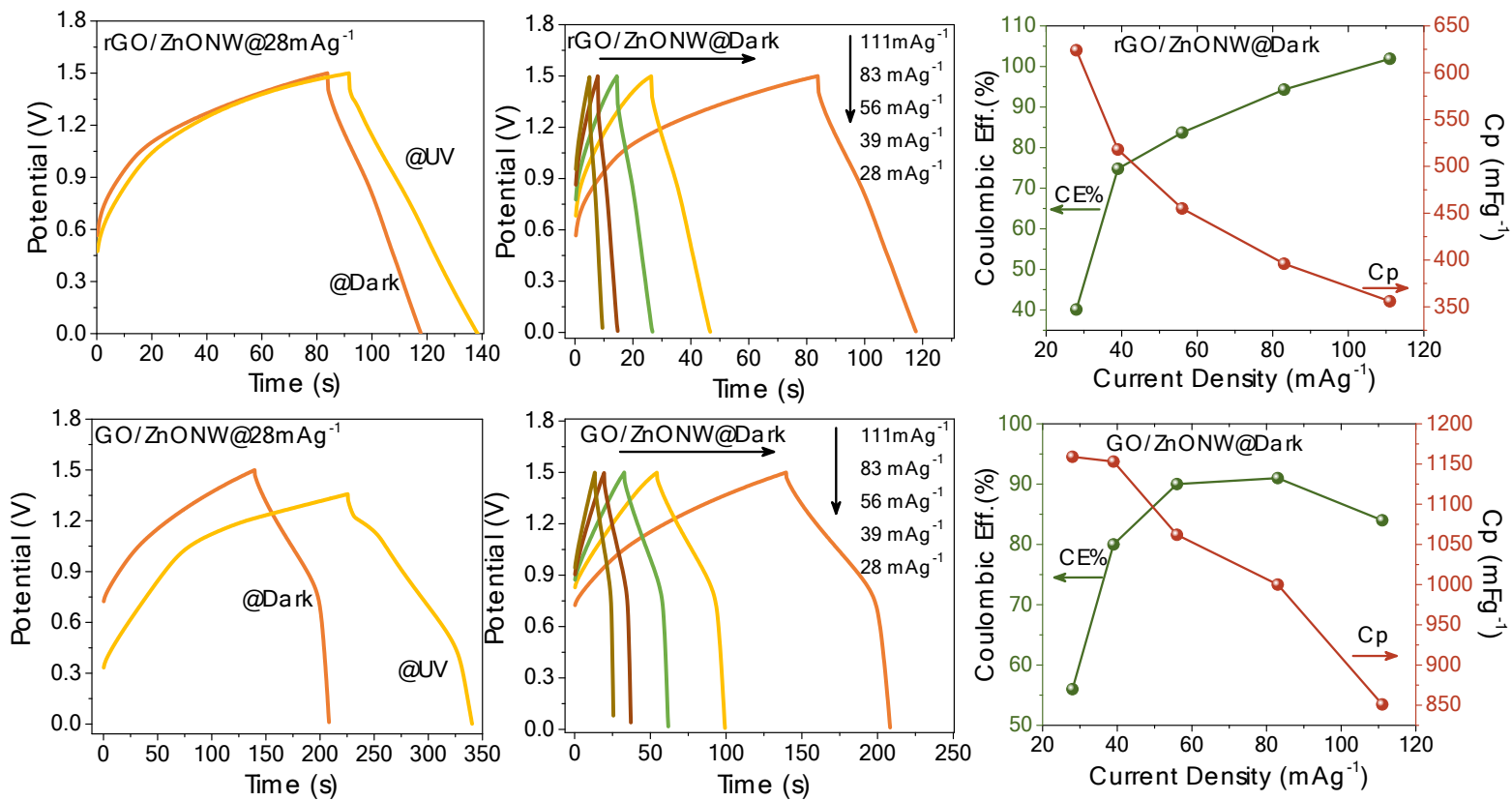


Figure S5. GCD curves and specific capacitance and CE% values of the composite PSC devices at various current densities under UV and in the dark.

GCD curves at lower current densities for composite PSCs

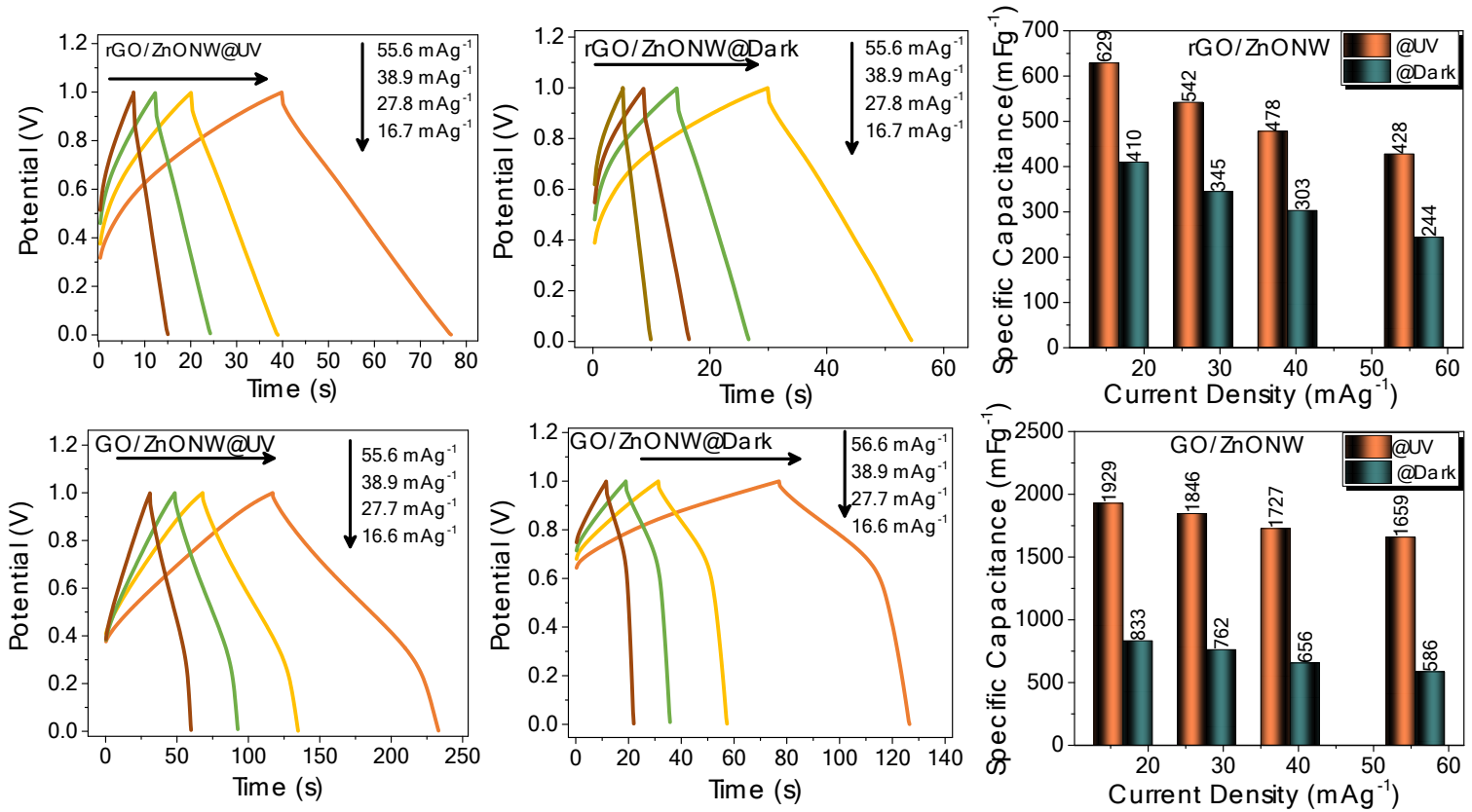


Figure S6. GCD curves and C_p values of the prepared PSC devices at various current densities obtained for the potential of 1V

Table S1. Comparison table for the performances of the PSC devices prepared from various photoelectrode materials.

| PSC Device | Specific Capacitance | Current density | Energy density | Cycle number/ Cp Retention(%) | Ref./Year |
|--|--------------------------|-------------------------|--------------------------|----------------------------------|-----------|
| GO/ZnONW | 2200 mFg ⁻¹ | 0.11 Ag ⁻¹ | 2.5Whkg ⁻¹ | 5k/99.8 | This work |
| rGO/ZnONW | 880 mFg ⁻¹ | 0.11 Ag ⁻¹ | 1.0Whkg ⁻¹ | 5k/99.5 | This work |
| Cu@Cu ₂ O (NPC@Cu ₂ O)* | 782 Fg ⁻¹ | 1.0 Ag ⁻¹ | NA | 10k/99.5 | S1/2019 |
| ITO/P3HT | 2.44 mF/cm ⁻² | 0.02 mAcm ⁻² | NA | NA | S2/2021 |
| C/PAAQ//PAAQ/C | 53 mF/cm ⁻² | 0.5 mAcm ⁻² | 5μWhcm ⁻² | 4k/90.0 | S3/2020 |
| CoS//AC | 30 Fg ⁻¹ | 2.0 Ag ⁻¹ | 15.58 Whkg ⁻¹ | 2k/97.9 | S4/2019 |
| Co ₃ O ₄ /g-C ₃ N ₄ | 64.3 mF/cm ⁻² | 26.6 mAcm ⁻² | 12.9 Whkg ⁻¹ | 5k/83.3 | S5/2020 |
| BiVO ₄ -RGO* | 141.8 Fg ⁻¹ | 0.2 Ag ⁻¹ | 4.1 mAh.g ⁻¹ | 110/80.0 | S6/2020 |
| NiCo ₂ O ₄ /ZnO//NiCo ₂ O ₄ /ZnO | 25 mFg ⁻¹ | 0.5 mAcm ⁻² | 1.35mWhkg ⁻¹ | 2k/97.0 | S7/2017 |
| Bi ₂ O ₃ -Fe ₃ O ₄ * | 306.6 Fg ⁻¹ | 1.0 Ag ⁻¹ | NA | 1k/60.0 | S8/2021 |

*Liquid electrolyte system

EIS analysis

Table S2. EIS parameters of the composite PSC under UV irradiation and at dark.

| Device | UV-light | R1 (Ω) | R2 (Ω) | R3 (Ω) | C3 (mF) | a1 | W (Ωs ^{-1/2}) |
|------------|----------|--------|--------|--------|-----------------------|-------|-------------------------|
| GO/ZnO NW | off | 42.6 | 330.5 | -260 | 3.9 | 0.895 | 1001 |
| | on | 24.5 | 401.4 | 227.1 | 62.6x10 ⁻³ | 0.814 | 510.8 |
| rGO/ZnO NW | off | 39.9 | 43.3 | 5024 | 7.6 | 0.913 | 240.9 |
| | on | 39.1 | 19.9 | 1462 | 13.0 | 0.924 | 126.3 |

References

- S1. C. An, Z. Wang, W. Xi, K. Wang, X. Liu, and Yi Ding, Nanoporous Cu@Cu₂O hybrid arrays enable photoassisted supercapacitor with enhanced capacities, *J. Mater. Chem. A*, 2019, 7, 15691–15697
- S2. W. J. Dong, W. S. Cho, and J.-L. Lee, Indium Tin Oxide Branched Nanowire and Poly(3-hexylthiophene)Hybrid Structure for a Photorechargeable Supercapacitor, *ACS Appl. Mater. Interfaces* 2021, 13, 22676 – 22683

- S3. A.Das, S. Deshagani, P. Ghosal, M. Deepa, Redox active and electrically conducting cobalt telluride Nanorods/Poly(1 aminoanthraquinone) composite and photoactive Rose Bengal dye based photo-supercapacitor, Applied Material Today 19(2020)100592
- S4. K Ashok Kumar, A Pandurangan, S Arumugam and M. Sathiskumar, Effect of Bi-functional Hierarchical Flower-like CoS Nanostructure on its Interfacial Charge Transport Kinetics, Magnetic and Electrochemical Behaviors for Supercapacitor and DSSC Applications, *Scientific Reports*, **9**, 1228 (2019)
- S5. Liqi Bai,Hongwei Huang,Songge Zhang, Lin Hao,Zhili Zhang,Hongfen Li, Li Sun, Lina Guo,Haitao Huang,Yihe Zhang, Photocatalysis-Assisted Co₃O₄/g-CN p–n Junction All-Solid-State Supercapacitors: A Bridge between Energy Storage and Photocatalysis, *Adv. Sci.* 2020, **7**, 2001939
- S6. A. Roy, P. Majumdar, A photoelectrochemical supercapacitor based on a single BiVO₄-RGO bilayer photocapacitive electrode, *Electrochimica Acta* 329 (2020) 135170
- S7. B. D. Boruah, A. Misra, Photocharge-Enhanced Capacitive Response of a Supercapacitor, *Energy Technol.* 2017, **5**, 1356 – 1363
- S8. P. Pattananuwat, A. Khampuanbuta, H. Haromae, Novel electrode composites of mixed bismuth-iron oxide / graphene utilizing for photo assisted supercapacitors, *Electrochimica Acta* 370 (2021) 137741